01 Jan 1980

Combined Heat And Lass Transfer In Mixed Confection Ower A Horizontal Flat Plate

T. S. Chen
Missouri University of Science and Technology, tschen@mst.edu

F. A. Strobel

Recommended Citation

T. S. Chen and F. A. Strobel, "Combined Heat And Lass Transfer In Mixed Confection Ower A Horizontal Flat Plate," *Journal of Heat Transfer*, vol. 102, no. 3, pp. 538 - 543, American Society of Mechanical Engineers, Jan 1980.
The definitive version is available at https://doi.org/10.1115/1.3244337

Combined Heat and Mass Transfer in Mixed Convection over a Horizontal Flat Plate

T. S. Chen
Mem. ASME

F. A. Strobel[1]

Department of Mechanical and Aerospace Engineering, University of Missouri-Rolla, Rolla, MO 65401

The combined effects of buoyancy forces from thermal and species diffusion on the heat and mass transfer characteristics are analyzed for laminar boundary layer flow over a horizontal flat plate. The analysis is restricted to processes with low concentration levels such that the interfacial velocities due to mass diffusion and the diffusion-thermo/thermo-diffusion effects can be neglected. Numerical results for friction factor, Nusselt number, and Sherwood number are presented for gases having a Prandtl number of 0.7, with Schmidt numbers ranging from 0.6 to 2.0. In general, it is found that, for the thermally assisting flow, the surface heat and mass transfer rates as well as the wall shear stress increase with increasing thermal buoyancy force. These quantities are further enhanced when the buoyancy force from species diffusion assists the thermal buoyancy force, but are reduced when the two buoyancy forces oppose each other. While a higher heat transfer rate is found to be associated with a lower Schmidt number, a higher mass transfer rate occurs at a higher Schmidt number.

Introduction

In studying forced convective heat transfer over horizontal surfaces, the buoyancy effect may become significant if the flow velocities are relatively low and the temperature and/or concentration differences between the surface and the free stream are large. This is because the buoyancy forces induce a streamwise pressure gradient which modifies the flow field and hence the heat and mass transfer rates. Thus, it is of practical interest to study the heat and mass transfer characteristics in flow situations in which the buoyancy effects from both thermal and species diffusions are significant. Even in processes with very low concentration levels, such as terrestrial processes in air and in water, the buoyancy effect from species diffusion can play a role as important as the thermal buoyancy effect. Atmospheric flows, for example, are not only influenced by the temperature difference between the surface of the earth and the ambient air, but also by the amount of water vapor that is diffused from the ground into the air. If the concentration level is low, the analysis of the problem can be greatly simplified by neglecting the interfacial velocities due to species diffusion as well as the diffusion-thermo and thermo-diffusion effects (i.e., the Soret and Dufour effects).

Thermal buoyancy effects in laminar forced convection flow over a horizontal flat plate have been analyzed rather extensively (see, for example, [1–3]). An analysis dealing with the combined heat and mass transfer in natural convection flow over a horizontal plate has also been reported [4]. However, a study of mixed forced and natural convection flow over a horizontal plate under the combined buoyancy effects of thermal and mass diffusion seems not to have been reported in the literature. This has motivated the present investigation. In the analysis, consideration is given to processes with low concentration levels. The conservation equations of the boundary layer are reduced to a dimensionless form by a nonsimilarity transformation, and the resulting system of equations are then solved by the local nonsimilarity method (see, for example, [5, 6]).

Numerical results are obtained for a Prandtl number of 0.7, which is representative of air, and Schmidt numbers Sc of 0.6, 1.0, and 2.0. The parameter N which measures the relative effect of mass and thermal diffusion ranges from −0.5 to 2.0 for Schmidt number of 0.6 and from −0.5 to 1.0 for Sc = 1.0 and 2.0. For each case the thermal buoyancy parameter $\mathrm{Gr}_x/\mathrm{Re}_x^{5/2}$ is varied from 0 to 1.0. The Schmidt number range covers diffusion into air of water vapor (Sc = 0.6), carbon dioxide (Sc = 0.94), methanol (Sc = 0.97), benzene (Sc = 1.76), and ethyl benzene (Sc = 2.01), etc. under one atmospheric pressure and room temperature.

Analysis

Consider a horizontal flat plate which is placed parallel to a uniform free stream with velocity u_∞, temperature T_∞, and mass fraction C_∞. The plate is maintained at a uniform temperature T_w and uniform mass fraction C_w. Let x represent the streamwise distance from the leading edge of the plate and y the distance normal to the plate. Positive y is taken vertically upward for flow above the plate and vertically downward for flow below the plate.

With the assumption of constant fluid properties, the Boussinesq approximation, and in the absence of Soret and Dufour effects, the conservation equations of the laminar boundary layer can be written as

$$\frac{\partial u}{\partial x}+\frac{\partial v}{\partial y}=0 \tag{1}$$

$$u\frac{\partial u}{\partial x}+v\frac{\partial u}{\partial y}=\nu\frac{\partial^2 u}{\partial y^2}\pm g\beta\frac{\partial}{\partial x}\int_y^\infty (T-T_\infty)dy \pm g\beta^*\frac{\partial}{\partial x}\int_y^\infty (C-C_\infty)dy \tag{2}$$

$$u\frac{\partial T}{\partial x}+v\frac{\partial T}{\partial y}=\alpha\frac{\partial^2 T}{\partial y^2} \tag{3}$$

$$u\frac{\partial C}{\partial x}+v\frac{\partial C}{\partial y}=D\frac{\partial^2 C}{\partial y^2} \tag{4}$$

The second and third terms on the right-hand side of equation (2) are, respectively, the pressure gradients induced by the buoyancy forces due to thermal and mass diffusion. The plus and minus signs preceding these terms pertain to flows above and below the plate, respectively. Equations (1–3) are subject to the following boundary conditions.

$$u=0,\ v=v_w,\ T=T_w,\ C=C_w \text{ at } y=0$$

$$u\to u_\infty,\ T\to T_\infty,\ C\to C_\infty \text{ as } y\to\infty \tag{5}$$

To solve equations (1–4) by the local nonsimilarity method, it is necessary to make a transformation from the (x, y) coordinates to the $(\xi(x), \eta(x, y))$ coordinates by introducing

$$\xi=\xi(x),\ \eta=y(u_\infty/\nu x)^{1/2} \tag{6}$$

[1] Presently with Naval Weapons Center, China Lake, Calif.

Contributed by The Heat Transfer Division and presented at the Winter Annual Meeting, New York, NY. December 2–7, 1979 of THE AMERICAN SOCIETY OF MECHANICAL ENGINEERS. Revised manuscript received by the Heat Transfer Division October 19, 1979.

In addition, one introduces a reduced stream function $F(\xi, \eta)$, a dimensionless temperature $\theta(\xi, \eta)$, and a dimensionless mass fraction $\lambda(\xi, \eta)$ defined, respectively, as

$$F(\xi, \eta) = \psi(x, y)/(\nu u_\infty x)^{1/2},\ \theta(\xi, \eta) = (T - T_\infty)/(T_w - T_\infty),$$
$$\lambda(\xi, \eta) = (C - C_\infty)/(C_w - C_\infty) \quad (7)$$

where the stream function $\psi(x, y)$ satisfies the continuity equation (1) with

$$u = \partial\psi/\partial y,\ v = -\partial\psi/\partial x \quad (8)$$

By substituting equations (6) and (7) into equations (2–5), one obtains the following system of equations.

$$F''' + \frac{1}{2}FF'' \pm \frac{1}{2}\xi\left[\eta\theta + \int_\eta^\infty \theta d\eta + \xi\int_\eta^\infty \frac{\partial\theta}{\partial\xi}d\eta\right] \pm \frac{1}{2}N\xi$$
$$\times\left[\eta\lambda + \int_\eta^\infty \lambda d\eta + \xi\int_\eta^\infty \frac{\partial\lambda}{\partial\xi}d\eta\right] = \frac{1}{2}\xi\left[F'\frac{\partial F'}{\partial\xi} - F''\frac{\partial F}{\partial\xi}\right] \quad (9)$$

$$\frac{1}{\mathrm{Pr}}\theta'' + \frac{1}{2}F\theta' = \frac{1}{2}\xi\left[F'\frac{\partial\theta}{\partial\xi} - \theta'\frac{\partial F}{\partial\xi}\right] \quad (10)$$

$$\frac{1}{\mathrm{Sc}}\lambda'' + \frac{1}{2}F\lambda' = \frac{1}{2}\xi\left[F'\frac{\partial\lambda}{\partial\xi} - \lambda'\frac{\partial F}{\partial\xi}\right] \quad (11)$$

$$F(\xi, 0) + \xi\partial F(\xi, 0)/\partial\xi = 0,\ F'(\xi, 0) = 0,$$
$$\theta(\xi, 0) = 1,\ \lambda(\xi, 0) = 1 \quad (12a)$$

$$F'(\xi, \infty) = 1,\ \theta(\xi, \infty) = 0,\ \lambda(\xi, \infty) = 0 \quad (12b)$$

In the preceding equations the primes denote partial differentiation with respect to η, the thermal buoyancy parameter $\xi(x)$ is given by

$$\xi(x) = |\mathrm{Gr}_x|/\mathrm{Re}_x^{5/2} \quad (13)$$

and the relative effect between species and thermal diffusion N by

$$N = \beta^*(C_w - C_\infty)/\beta(T_w - T_\infty) = \mathrm{Gr}_{x,c}/\mathrm{Gr}_x \quad (14)$$

in which the local thermal Grashof number Gr_x, the local concentration Grashof number $\mathrm{Gr}_{x,c}$, and the local Reynolds number are defined as

$$\mathrm{Gr}_x = g\beta(T_w - T_\infty)x^3/\nu^2,$$
$$\mathrm{Gr}_{x,c} = g\beta^*(C_w - C_\infty)x^3/\nu^2,\ \mathrm{Re}_x = u_\infty x/\nu \quad (15)$$

The buoyancy force from species diffusion assists the thermal buoyancy force when $N > 0$, whereas it opposes the thermal buoyancy force when $N < 0$. The case of $N = 0$ corresponds to the situation in which there is no buoyancy force from species diffusion.

It is noted here that the absolute value is used in the definition of the thermal buoyancy parameter ξ. Thus, the plus and minus signs on the left-hand side of equation (9) refer, respectively, to thermal buoyancy force assisting and opposing the forced flow. For flow above the plate, the plus sign is associated with the case $T_w > T_\infty$, and the minus sign with the case $T_w < T_\infty$. The opposite is true for flow below the plate.

In writing the boundary condition $F(\xi, 0) + \xi\,\partial F(\xi, 0)/\partial\xi = 0$ in equation (12a), it has been assumed that the normal velocity at the wall v_w due to mass diffusion is negligibly small. This assumption is valid when the condition

$$2(v_w x/\nu)/(u_\infty x/\nu)^{1/2} \ll 1 \quad (16)$$

is fulfilled. Since $v_w = -[D/(1 - C_w)](\partial C/\partial y)_{y=0}$ (see, for example, [7]), the above condition is equivalent to

$$\frac{2}{\mathrm{Sc}}\frac{C_w - C_\infty}{1 - C_w}[-\lambda'(\xi, 0)] \ll 1 \quad (17)$$

Equation (17) will be valid when the ratio $(C_w - C_\infty)/(1 - C_w)$ is very small; that is, when the mass-fraction level is very low. There are many transport processes in which the mass-fraction level is low, but the species diffusion effect is significant. The evaporation of water vapor into an air stream is such an example. Simple calculations for diffusion of water vapor into air at one atmospheric pressure and around room temperature (with Pr = 0.7 and Sc = 0.6) show that $C < 0.04$ for $T < 100°\mathrm{F}$ and that $(C_w - C_\infty) \doteq 0.0057 \sim 0.0294$, $(C_w - C_\infty)/(1 - C_w) \doteq 0.006 \sim 0.03$, and $N \doteq 1 \sim 4$ for $(T_w - T_\infty) = 20 \sim 40°\mathrm{F}$. Thus, even though the mass-fraction C and the mass-fraction difference $(C_w - C_\infty)$ are small, the buoyancy effects from mass diffusion are as significant as the thermal buoyancy effects (i.e., $N > 1$). In addition, for $N \leq 2$ and $\mathrm{Gr}_x/\mathrm{Re}_x^{5/2} = 0 \sim 1.0$, as covered in the present study, the value of $2(C_w - C_\infty)[-\lambda'(\xi, 0)]/[\mathrm{Sc}(1 - C_w)]$ varies from about 0.005 to 0.025, which is indeed very small compared to 1. Thus, the condition for the neglect of interfacial velocity, as given by equation (17), is fully satisfied for such a flow process and can also be satisfied for similar processes with low mass-fraction levels. Furthermore, with the existence of small C and $(C_w - C_\infty)$ values, the neglect of Soret and Dufour effects in the analysis can be justified. The effects of finite and large interfacial velocities (i.e., large values of $(C_w - C_\infty)/(1 - C_w)$) on mass transfer in laminar boundary flows were examined by Acrivos [8, 9].

To solve equations (9–12) by the local nonsimilarity method, it is first necessary to remove the integral terms in equation (9) by differentiating the equation once with respect to η. This yields a fourth order differential equation and necessitates the introduction of an

Nomenclature

C = mass fraction or concentration
C_f = local friction factor
D = mass diffusion coefficient
F = reduced stream function
G = derivative of F with respect to ξ
g = gravitational acceleration
Gr_x = local thermal Grashof number, $g\beta(T_w - T_\infty)x^3/\nu^2$
Gr_L = thermal Grashof number based on L, $g\beta(T_w - T_\infty)L^3/\nu^2$
$Gr_{x,c}$ = local concentration Grashof number, $g\beta^*(C_w - C_\infty)x^3/\nu^2$
h = local heat transfer coefficient
$\overline{h}$ = average heat transfer coefficient
h_m = local mass transfer coefficient
$\overline{h}_m$ = average mass transfer coefficient
k = thermal conductivity
L = length of plate
$\dot{m}_w$ = local surface mass transfer rate per unit area
N = ratio of Grashof numbers, $\mathrm{Gr}_{x,c}/\mathrm{Gr}_x = \beta^*(C_w - C_\infty)/\beta(T_w - T_\infty)$
Nu_x = local Nusselt number, $q_w x/(T_w - T_\infty)k$
$\overline{\mathrm{Nu}}$ = average Nusselt number, $\overline{h}L/k$
Pr = Prandtl number
q_w = local surface heat transfer rate per unit area
Re_x = local Reynolds number, $u_\infty x/\nu$
Re_L = Reynolds number based on L, $u_\infty L/\nu$
Sc = Schmidt number
Sh_x = local Sherwood number, $\dot{m}_w x/\rho D(C_w - C_\infty)$
$\overline{\mathrm{Sh}}$ = average Sherwood number, $\overline{h}_m L/\rho D$
T = fluid temperature
u = axial velocity component
v = normal velocity component
x = axial coordinate
y = transverse coordinate
α = thermal diffusivity
β = volumetric coefficient of thermal expansion
β^* = volumetric coefficient of expansion with mass fraction
η = pseudo-similarity variable
θ = dimensionless temperature
λ = dimensionless mass fraction
μ = dynamic viscosity
ν = kinematic viscosity
ξ = thermal buoyancy parameter
ξ_L = thermal buoyancy parameter based on L
ρ = density of fluid
τ_w = wall shear stress
ϕ = derivative of θ with respect to ξ
ψ = stream function
ω = derivative of λ with respect to ξ

Subscripts

w = condition at wall
∞ = condition at free stream

additional boundary condition, which can be obtained by evaluating equation (9) at $\eta = 0$. If, in addition, one introduces the dependent variables

$$G = \partial F/\partial \xi,\ \phi = \partial \theta/\partial \xi,\ \omega = \partial \lambda/\partial \xi \tag{18}$$

the resulting system of equations can be written as

$$F'''' + \frac{1}{2}(FF''' + F'F'') \pm \frac{1}{2}\xi\eta(\theta' + N\lambda') \mp \frac{1}{2}\xi^2(\phi + N\omega) = \frac{1}{2}\xi(F'G'' - F'''G) \tag{19}$$

$$\frac{1}{\mathrm{Pr}}\theta'' + \frac{1}{2}F\theta' = \frac{1}{2}\xi(F'\phi - \theta'G) \tag{20}$$

$$\frac{1}{\mathrm{Sc}}\lambda'' + \frac{1}{2}F\lambda' = \frac{1}{2}\xi(F'\omega - \lambda'G) \tag{21}$$

$$F(\xi, 0) + \xi G(\xi, 0) = F'(\xi, 0) = 0,\ \theta(\xi, 0) = \lambda(\xi, 0) = 1 \tag{22a}$$

$$F'''(\xi, 0) = \mp\frac{1}{2}\xi\left[\int_0^\infty \theta d\eta + N\int_0^\infty \lambda d\eta\right] \mp \frac{1}{2}\xi^2\left[\int_0^\infty \phi d\eta + N\int_0^\infty \omega d\eta\right] \tag{22b}$$

$$F'(\xi, \infty) = 1,\ \theta(\xi, \infty) = \lambda(\xi, \infty) = 0 \tag{22c}$$

Equations (19–21) are three coupled equations with six unknown functions $F, \theta, \lambda, G, \phi$, and ω. In order to solve these equations by the local nonsimilarity method, it is necessary to obtain subsidiary equations by differentiating equations (19–21) with respect to ξ. In the present investigation, this differentiation is carried out once and the analysis corresponds therefore to the second level of truncation [5, 6]. For the second level of truncation, the transformed conservation equations are left intact, but terms containing $\partial G/\partial\xi$, $\partial\phi/\partial\xi$, $\partial\omega/\partial\xi$ and their η derivatives are neglected in the subsidiary equations. With this operation, the system of equations for the second level of truncation can be summarized as follows.

(a) Equations (19–21)

(b) The truncated equations for G, ϕ, and ω given by

$$G'''' + \frac{1}{2}(FG''' + F''G') + F'''G \pm \frac{1}{2}\eta[\theta' + \xi\phi' + N(\lambda' + \xi\omega')] \mp \xi(\phi + N\omega) + \frac{1}{2}\xi(GG''' - G'G'') = 0 \tag{23}$$

$$\frac{1}{\mathrm{Pr}}\phi'' + \frac{1}{2}F\phi' - \frac{1}{2}F'\phi + G\theta' + \frac{1}{2}\xi(G\phi' - G'\phi) = 0 \tag{24}$$

$$\frac{1}{\mathrm{Sc}}\omega'' + \frac{1}{2}F\omega' - \frac{1}{2}F'\omega + G\lambda' + \frac{1}{2}\xi(G\omega' - G'\omega) = 0 \tag{25}$$

(c) The boundary conditions

$$F(\xi, 0) = F'(\xi, 0) = G(\xi, 0) = G'(\xi, 0) = \phi(\xi, 0) = \omega(\xi, 0) = 0$$
$$\theta(\xi, 0) = \lambda(\xi, 0) = 1 \tag{26a}$$

$$F'''(\xi, 0) = \mp\frac{1}{2}\xi\left[\int_0^\infty \theta d\eta + N\int_0^\infty \lambda d\eta\right] \mp \frac{1}{2}\xi^2\left[\int_0^\infty \phi d\eta + N\int_0^\infty \omega d\eta\right] \tag{26b}$$

$$G'''(\xi, 0) = \mp\frac{1}{2}\left[\int_0^\infty \theta d\eta + N\int_0^\infty \lambda d\eta\right] \mp \frac{3}{2}\xi\left[\int_0^\infty \phi d\eta + N\int_0^\infty \omega d\eta\right] \tag{26c}$$

$$F'(\xi, \infty) = 1,\ G'(\xi, \infty) = \theta(\xi, \infty) = \phi(\xi, \infty) = \lambda(\xi, \infty) = \omega(\xi, \infty) = 0 \tag{26d}$$

It can be seen that equations (19–21) and (23–25) are coupled and must be solved simultaneously to obtain solutions for the unknown functions of $F, \theta, \lambda, G, \phi$, and ω. This will be described later.

The physical quantities of greatest interest are the local and average Nusselt numbers Nu_x and $\overline{\mathrm{Nu}}$, the local and average Sherwood numbers Sh_x and $\overline{\mathrm{Sh}}$, and the local friction factor C_f. The local quantities are defined, respectively, by

$$\mathrm{Nu}_x = \frac{q_w}{T_w - T_\infty}\frac{x}{k},\ \mathrm{Sh}_x = \frac{\dot{m}_w}{C_w - C_\infty}\frac{x}{\rho D},\ C_f = \frac{\tau_w}{\rho u_\infty{}^2/2} \tag{27}$$

With the use of Fourier's law $q_w = -k(\partial T/\partial y)_{y=0}$, Fick's law $\dot{m}_w = -\rho D(\partial C/\partial y)_{y=0}$, and the definition of wall shear stress $\tau_w = \mu(\partial u/\partial y)_{y=0}$ along with equations (6) and (7), the following expressions for the local Nusselt number, the local Sherwood number, and the local friction factor are obtained.

$$\mathrm{Nu}_x\mathrm{Re}_x{}^{-1/2} = -\theta'(\xi, 0),\ \mathrm{Sh}_x\mathrm{Re}_x{}^{-1/2} = -\lambda'(\xi, 0),\ C_f\mathrm{Re}_x{}^{1/2} = 2F''(\xi, 0) \tag{28}$$

The average Nusselt and Sherwood numbers are defined, respectively, by

$$\overline{\mathrm{Nu}} = \bar{h}L/k,\ \overline{\mathrm{Sh}} = \bar{h}_m L/\rho D \tag{29}$$

where the average heat transfer and mass transfer coefficients are determined from the following expressions

$$\bar{h} = \frac{1}{L}\int_0^L h(x)dx,\ \bar{h}_m = \frac{1}{L}\int_0^L h_m(x)dx \tag{30}$$

When the axial coordinate x in equation (30) is replaced by the thermal buoyancy parameter ξ, the average Nusselt and Sherwood numbers are found to be

$$\overline{\mathrm{Nu}}\mathrm{Re}_L{}^{-1/2} = \frac{2}{\xi_L}\int_0^{\xi_L}[-\theta'(\xi, 0)]d\xi \tag{31}$$

$$\overline{\mathrm{Sh}}\mathrm{Re}_L{}^{-1/2} = \frac{2}{\xi_L}\int_0^{\xi_L}[-\lambda'(\xi, 0)]d\xi \tag{32}$$

wherein the thermal buoyancy parameter ξ_L, the Reynolds number Re_L, and the Grashof number Gr_L are based on the plate length and are expressed, respectively, by

$$\xi_L = \mathrm{Gr}_L/\mathrm{Re}_L{}^{5/2},\ \mathrm{Re}_L = u_\infty L/\nu,\ \mathrm{Gr}_L = g\beta(T_w - T_\infty)L^3/\nu^2 \tag{33}$$

Also of interest are the velocity, temperature, and concentration distributions. They are determined, respectively, from the following expressions.

$$u/u_\infty = F'(\xi, \eta),\ (T - T_\infty)/(T_w - T_\infty) = \theta(\xi, \eta),\ (C - C_\infty)/C_w - C_\infty) = \lambda(\xi, \eta) \tag{34}$$

Numerical Solutions

Equations (19–21) and (23–25) can be treated as a system of coupled ordinary differential equations for a prescribed value of ξ. These equations were solved by the Runge-Kutta integration scheme in conjunction with Newton-Raphson shooting method to fulfill the conditions at the edge of the boundary layers. A predictor-corrector integration scheme was employed to improve the accuracy of the numerical integration.

The procedure for solving the system of equations for a prescribed value of ξ is similar to that described in [1]. The initial values which must be guessed are $F''(\xi, 0)$, $G''(\xi, 0)$, $\theta'(\xi, 0)$, $\phi'(\xi, 0)$, $\lambda'(\xi, 0)$, $\omega'(\xi, 0)$ as well as the θ, ϕ, λ, and ω integrals. The integrals were considered converged when the differences in the values of $F''(\xi, 0)$ and $G''(\xi, 0)$ between the two successive iterations became less than 10^{-4} and 10^{-3}, respectively. A solution was considered converged when the conditions $|F' - 1.0, F''| \le 3 \times 10^{-3}$, $|\theta, \theta', \lambda, \lambda', \phi, \phi', \omega, \omega'| \le 5 \times 10^{-3}$, and $|G', G''| \le 10^{-2}$ at the edge of the boundary layers were fulfilled simultaneously.

Results and Discussion

Numerical results were obtained for a Prandtl number of 0.7 and Schmidt numbers of 0.6, 1.0, and 2.0. For a Schmidt number of 0.6, the values of N cover 2.0, 1.0, 0.5, 0, −0.5 and for Schmidt numbers of 1.0 and 2.0 they cover 1.0, 0.5, 0, −0.5. For each case the thermal buoyancy parameter $\mathrm{Gr}_x/\mathrm{Re}_x{}^{5/2}$ was varied from 0 to 1.0; that is, the

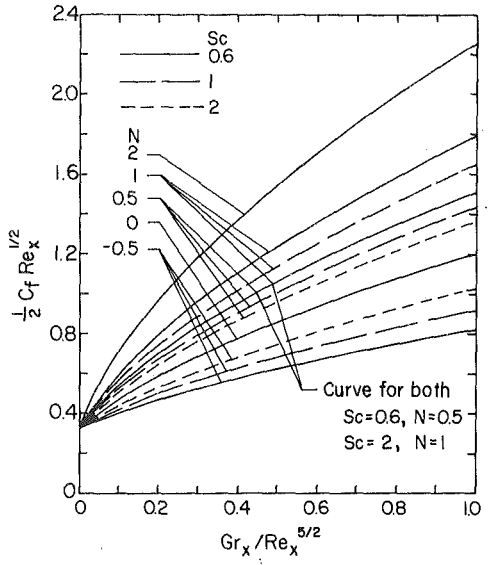

Fig. 1 Local friction factor results

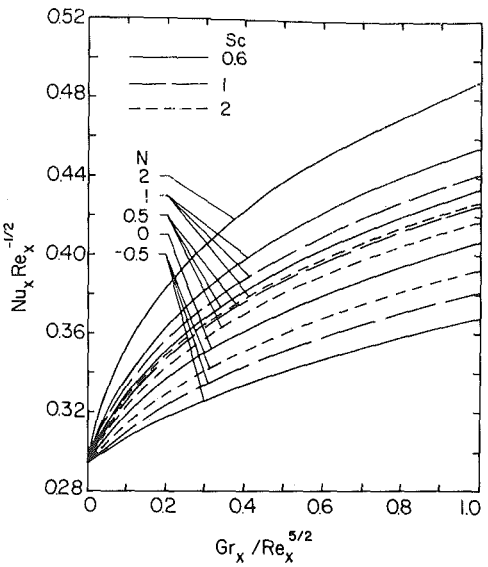

Fig. 2 Local Nusselt number results

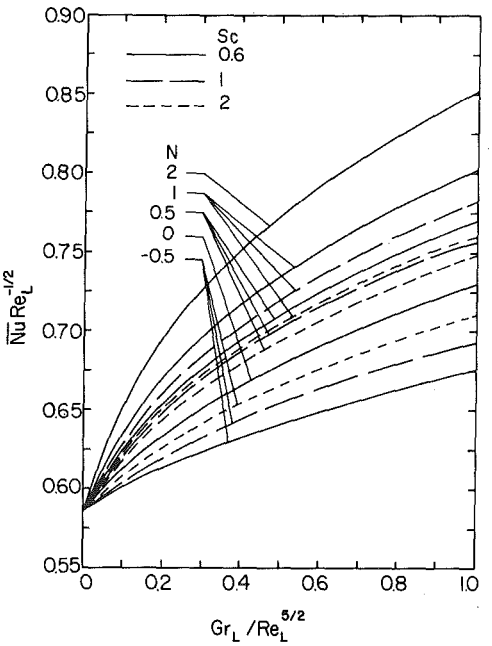

Fig. 3 Average Nusselt number results

results are for thermal buoyancy force assisting the forced flow. These results will now be presented.

The effects of buoyancy forces on the local friction factor, the local Nusselt number, and the average Nusselt number are shown, respectively, in Figs. 1–3. As can be seen from the figures, the local friction factor and the local Nusselt number increase with increasing value of $Gr_x/Re_x^{5/2}$, whereas the average Nusselt number increase with increasing $Gr_L/Re_L^{5/2}$. This trend is to be expected, because the favorable pressure gradient caused by the buoyancy forces increases the flow velocity near the wall, which results in an increase in the wall shear stress and hence the rate of surface heat transfer. By comparing the curves with that for $N = 0$ (i.e., no buoyancy effect from mass diffusion), it is possible to measure the relative effect between the buoyancy forces from mass and thermal diffusion. For a given Schmidt number, the friction factor and the Nusselt numbers increase beyond those for $N = 0$ when $N > 0$; that is, when the buoyancy force from mass diffusion acts in the same direction as the thermal buoyancy force, thereby resulting in additive buoyancy effects. On the other hand, the two buoyancy forces oppose each other when $N < 0$. The net effect is a decrease in the combined buoyancy forces below that for $N = 0$ and hence a decrease in the friction factor and the Nusselt numbers. It is also of interest to note from Figs. 1 and 2 that a lower Schmidt number yields larger local friction factor and local Nusselt number than those for $N = 0$ when $N > 0$ and smaller local friction factor and local Nusselt number when $N < 0$. The reason for the larger departure of these two quantities from $N = 0$ is that a diffusing species with a smaller Schmidt number has a larger diffusion coefficient which exerts a larger effect on the flow and thermal fields.

The local Sherwood numbers are shown in Fig. 4 as a function of the thermal buoyancy parameter $Gr_x/Re_x^{5/2}$ and the average Sherwood numbers in Fig. 5 as a function of $Gr_L/Re_L^{5/2}$. Again, the curves for $N = 0$ correspond to the situation in which buoyancy effect from species diffusion does not exist. As expected, the effect of the buoyancy forces is to increase the flow velocity which in turn enhances the Sherwood number and hence the mass transfer rate. As in the local friction factor and Nusselt number results, the Sherwood numbers increase when $N > 0$ and decrease when $N < 0$. In addition, a larger Schmidt number is seen to provide a larger Sherwood number. This is because as the Schmidt number increases, the concentration boundary layer thickness decreases, thus resulting in a larger surface concentration gradient (see Fig. 8) and hence a higher rate of mass transfer from the surface.

It must be pointed out that as the value of N becomes more negative, the buoyancy effect due to mass diffusion may outweigh that due to thermal diffusion and the net effect of the buoyancy forces is to oppose the forced flow. To determine if the net buoyancy force effect will assist or oppose the forced flow, it is necessary to examine the last two terms on the left-hand side of equation (9),

$$\frac{1}{2}\xi\left[\eta\theta + \int_\eta^\infty \theta d\eta + \xi\int_\eta^\infty \frac{\partial\theta}{\partial\xi}d\eta\right]$$

and

$$\frac{1}{2}N\xi\left[\eta\lambda + \int_\eta^\infty \lambda d\eta + \xi\int_\eta^\infty \frac{\partial\lambda}{\partial\xi}d\eta\right].$$

For the case of Sc = Pr, the θ and λ solutions are identical. Thus, if $N = -1$, these terms will add up to zero and the buoyancy forces cancel each other, yielding results identical to those for pure forced convection. In general, for a given thermal buoyancy force, if the sum of the two terms is positive, the net buoyancy force will assist the forced flow. On the other hand, if it is negative, the net buoyancy force will oppose the forced flow. These outcomes depend on the Schmidt and Prandtl numbers as well as on the relative species-thermal buoyancy parameter N.

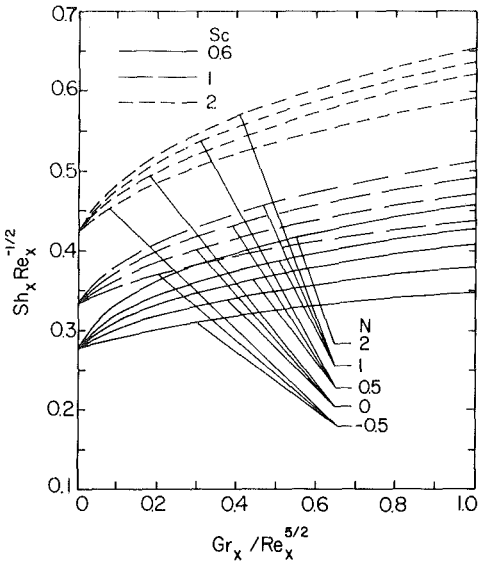

Fig. 4 Local Sherwood number results

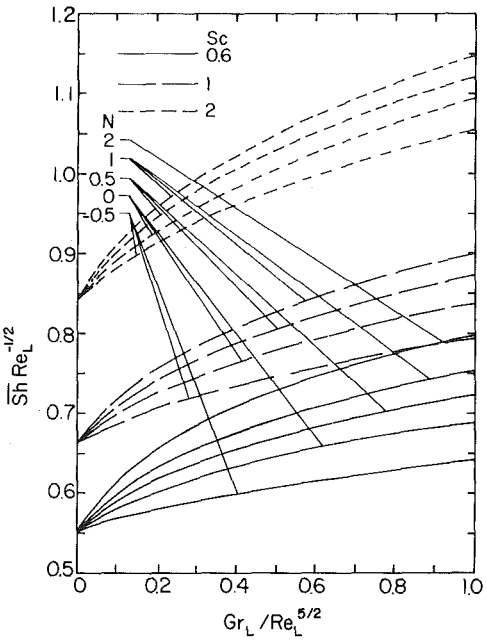

Fig. 5 Average Sherwood number results

It is interesting to examine how the buoyancy forces affect the velocity, temperature, and concentration fields in the boundary layers. Figure 6 shows representative velocity profiles for Schmidt numbers of 0.6 and 2.0. It is seen that for a given Schmidt number the velocity gradient at the wall increases as either $Gr_x/Re_x^{5/2}$ or N increases. In addition, for the same values of N and $Gr_x/Re_x^{5/2}$, a lower Schmidt number is seen to provide a larger wall velocity gradient. When the net buoyancy force becomes relatively large, the velocity profile exhibits an overshoot beyond the free stream velocity. This overshoot is more pronounced when the Schmidt number becomes smaller. For example, when $N = 1.0$ and $Gr_x/Re_x^{5/2} = 1.0$, the overshoot is about 37 percent for Sc = 0.6 as compared to about 20 percent for Sc = 2.0.

Representative temperature profiles are shown in Fig. 7 for Schmidt numbers of 0.6 and 2. The most noteworthy trends for a given Schmidt number are an increase in the temperature gradient at the wall and a decrease in the thermal boundary layer thickness as either N or $Gr_x/Re_x^{5/2}$ increases. In addition, the temperature gradient at the wall is seen to increase as the Schmidt number decreases.

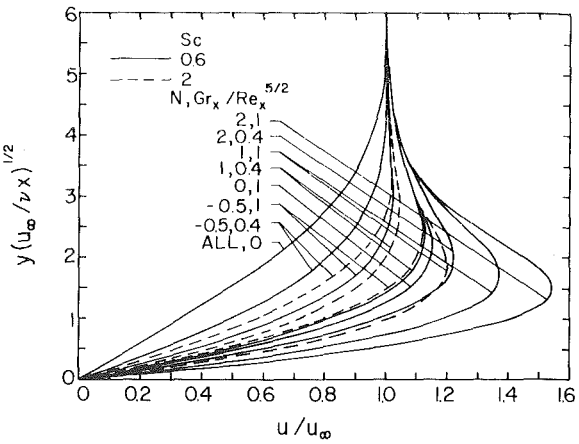

Fig. 6 Representative velocity profiles

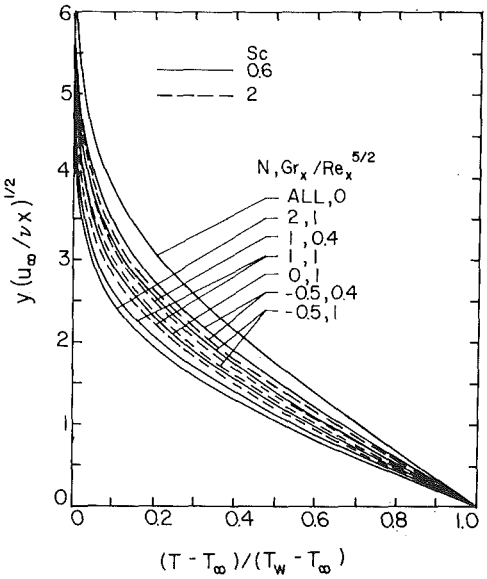

Fig. 7 Representative temperature profiles

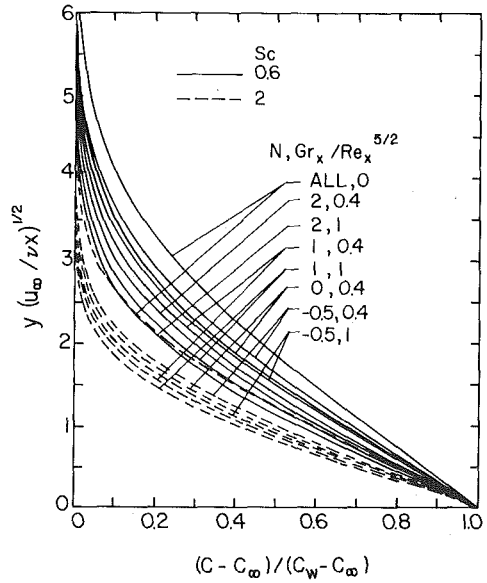

Fig. 8 Representative mass-fraction profiles

The mass fraction profiles (Fig. 8) exhibit trends similar to those of the temperature profiles. That is, the concentration gradient at the wall increases and the concentration boundary layer thickness decreases as the net buoyancy force increases. Also evident from the figure is that a larger wall gradient and a smaller boundary layer thickness are associated with a larger Schmidt number.

Conclusion

Laminar mixed convection flow over a horizontal flat plate under the combined buoyancy effects of thermal and mass diffusion has been studied analytically. The analysis is restricted to mass diffusion processes with low concentration levels, and numerical results are presented for a Prandtl number of 0.7, with Schmidt numbers of 0.6, 1.0, and 2.0. In general, it has been found that as the thermal buoyancy force increases (i.e., $Gr_x/Re_x^{5/2} > 0$ increases), the local surface heat and mass transfer rates as well as the local wall shear stress increase. When the buoyancy force from mass diffusion assists the thermal buoyancy force (i.e., when $N > 0$), these quantities increase further with an increasing value of N. On the other hand, they decrease with N when the two buoyancy forces oppose each other (i.e., when $N < 0$). While a higher heat transfer rate and a higher wall shear stress are associated with a lower Schmidt number, a higher mass transfer rate occurs at a higher Schmidt number. For relatively large net buoyancy forces that assist the forced flow, the velocity profiles exhibit an overshoot beyond the free stream velocity. This overshoot becomes more pronounced as the Schmidt number decreases.

Acknowledgment

This work was supported by a grant from the National Science Foundation (NSF ENG 75-15033 A01).

References

1 Chen, T. S., Sparrow, E. M. and Mucoglu, A., "Mixed Convection in Boundary Layer Flow on a Horizontal Plate," ASME JOURNAL OF HEAT TRANSFER, Vol. 99, 1977, pp. 66–71.

2 Sparrow, E. M., and Minkowycz, W. J., "Buoyancy Effects on Horizontal Boundary-Layer Flow and Heat Transfer," *International Journal of Heat and Mass Transfer*, Vol. 5, 1962, pp. 505–511.

3 Heiber, C. A., "Mixed Convection Above a Heated Horizontal Surface," *International Journal of Heat and Mass Transfer*, Vol. 16, 1973, pp. 769–785.

4 Pera, L., and Gebhart, B., "Natural Convection Flows Adjacent to Horizontal Surfaces Resulting from the Combined Buoyancy Effects of Thermal and Mass Diffusion," *International Journal of Heat and Mass Transfer*, Vol. 15, 1972, pp. 269–278.

5 Sparrow, E. M., and Yu, H. S., "Local Nonsimilarity Thermal Boundary-Layer Solutions," ASME JOURNAL OF HEAT TRANSFER, Vol. 93, 1971, pp. 328–334.

6 Chen, T. S., and Mucoglu, A., "Buoyancy Effects on Forced Convection Along a Vertical Cylinder," ASME JOURNAL OF HEAT TRANSFER, Vol. 97, 1975, pp. 198–203.

7 Eckert, E. R. G., and Drake, Jr., R. M., "*Heat and Mass Transfer*," Second Edition, Chapter 16, McGraw-Hill, New York, 1959.

8 Acrivos, A., "Mass Transfer in Laminar-Boundary-Layer Flows with Finite Interfacial Velocities," *AIChE Journal*, Vol. 6, 1960, pp. 410–414.

9 Acrivos, A., "The Asymptotic Form of the Laminar Boundary-Layer Mass-Transfer Rate for Large Interfacial Velocities," *Journal of Fluid Mechanics*, Vol. 12, 1962, pp. 337–357.